A Structural Damage Detection Technique Based

on Measured Frequency Response Functions

Mehdi Salehi

Department of Mechanical Engineering
Isfahan University of Technology, Isfahan, Iran
mehdi.salehi@me.iut.ac.ir

Saeed Ziaei-Rad

Department of Mechanical Engineering
Isfahan University of Technology, Isfahan, Iran

Mostafa Ghayour

Department of Mechanical Engineering
Isfahan University of Technology, Isfahan, Iran

Mohamad Ali Vaziri-Zanjani

Department of aerospace Engineering
Amirkabir University of Technology, Tehran, Iran

Abstract

Structural damage detection using vibration test data has been received great attention from many researchers in last few decades. Most of proposed methods yet, utilize extracted modal parameters or some indices constructed by these parameters. Few papers deal with application of Frequency Response Functions (FRFs) in structural damage detection. In this paper, a technique of damage detection based on real and imaginary parts of measured FRFs is presented. The method uses intact and damaged state information of structure so the need for analytical model is eliminated. Using real and imaginary residual FRF shape signals results in promising damage indicative features. A kind of abnormality is observed in residual FRF shapes in damaged sites which is detected via Gapped Smoothing Method (GSM). The method is demonstrated through some numerical and experimental case studies.

1 Introduction

Structural damage detection has gained increasing attention from researchers in last few decades. The drawbacks of traditional localized NDT methods such as high cost and long consuming time, has motivated development of global vibration based damage detection methods. All of these methods are based on variation of structural dynamic properties caused by damage. Sohn et al. provided a review on research advances in this area [14]. According to the process to treat the measured data, the vibration-based damage identification methods can be classified as model based and non-model based.

The model-based methods identify damage by correlating an analytical model, which is usually based on the finite element theory, with test modal data of the damaged structure [10], [4]. Comparisons of the updated model to the original one provide an indication of damage and further information on the damage location and its severity. However, the construction of the finite element model usually gives rise to model errors from simplified assumptions. To detect the damage, a high quality finite element model that could accurately predict the behavior of the intact structure is required but is often difficult to achieve.

Non model based damage detection methods are relatively straightforward. The changes of modal parameters between the intact and damaged states of the structure are directly used, or correlated with other relevant information, to develop the damage indicators for localizing damage in the structure. Early works of such methodologies make use of the natural frequency and mode shape information. Shifts in the natural frequencies [1], changes in the Modal Assurance Criteria (MAC) across substructures [15], changes in the COordinate Modal Assurance Criterion (COMAC) [5], changes in the Multiple Damage Location Assurance Criterion (MDLAC) [7] between the intact and damaged structure and changes in modal strain energy [12],[3] are formulated as indicators to localize damage. Pandy, Biswas and Samman further demonstrated that changes in mode shape curvature could be a good indicator of damage for beam-like structures [9].

A wide variety of non model based methods utilize modal parameters extracted from Frequency Response Functions (FRFs). Generally, using modal parameters contained spatial information, like mode shapes, results in more robust detection. Unfortunately, experimentally extracted mode shapes are often uncertain and inaccurate causing these methods less effective [2].

Perhaps, Maia, Silva and Sampaio were the first researchers that applied FRF data directly in damage detection problems [8]. They extended the mode shape curvature method to all frequencies in the measurement range and not just the modal frequencies. A 10 Degrees Of Freedom (DOF) lumped mass model was used to study the influence of frequency range, the input force location and noise

on the method [13]. They found that the influence of input force location is not important and the method is also of low sensitivity to noise. But the main drawback was that the method worked better for a frequency range before the first resonance or antiresonance, whichever comes first.

Liu, Lieven, and Ambrosio made use of residual imaginary part of FRF shapes to locate the structural damage [6]. They applied Gapped Smoothing Method (GSM) as well as Wavelet Transform (WT) to locate the abnormality caused by damage in a cantilever finite element model. The results were satisfactory over a wide frequency range.

Opposed to imaginary FRF shapes which poses their maxima at resonance frequencies, real part is zero at exact natural frequencies. Nevertheless the results based on real parts are damage indicative.

In this paper, both imaginary and real part of FRF shapes is used in damage detection. The theory was explained in details. Next, a clamped aluminum beam model is used to generate numerical simulated FRFs for healthy and damaged states which are then put into proposed methodology. Finally, an experimental response model of a steel beam is used to demonstrate the method experimental scheme.

2 Theory

The FRF of a n DOF system with structural damping is given by [11]

$$\alpha_{jk}(\omega) = \sum_{r=1}^{n} \frac{\phi_{jr}\phi_{kr}}{\omega_r^2 - \omega^2 + i\eta_r\omega_r^2} \tag{1}$$

where ϕ_{jr} is the j th element of r th structural mode shape, ω_r is the r th resonance frequency, η_r is the r th modal damping loss factor and ω is working frequency.

The k th FRF shape is defined as the deflection of the structure in measured degrees of freedom due to a unit harmonic excitation at k th degree of freedom.

$$\text{kth FRF shape at frequency} = \begin{Bmatrix} \alpha_{1k}(\omega) \\ \alpha_{2k}(\omega) \\ \vdots \\ \alpha_{nk}(\omega) \end{Bmatrix}$$

$$= \begin{Bmatrix} \dfrac{\phi_{11}\phi_{k1}}{\omega_1^2 - \omega^2 + i\eta_1\omega_1^2} + \cdots + \dfrac{\phi_{1n}\phi_{kn}}{\omega_n^2 - \omega^2 + i\eta_n\omega_n^2} \\ \dfrac{\phi_{21}\phi_{k2}}{\omega_1^2 - \omega^2 + i\eta_1\omega_1^2} + \cdots + \dfrac{\phi_{2n}\phi_{kn}}{\omega_n^2 - \omega^2 + i\eta_n\omega_n^2} \\ \vdots \\ \dfrac{\phi_{n1}\phi_{k1}}{\omega_1^2 - \omega^2 + i\eta_1\omega_1^2} + \cdots + \dfrac{\phi_{nn}\phi_{kn}}{\omega_n^2 - \omega^2 + i\eta_n\omega_n^2} \end{Bmatrix}$$

$$= \frac{\phi_{k1}}{\omega_1^2 - \omega^2 + i\eta_1\omega_1^2}\{\phi\}_1 + \cdots + \frac{\phi_{kn}}{\omega_n^2 - \omega^2 + i\eta_n\omega_n^2}\{\phi\}_n$$

$$= \sum_{r=1}^{n} \frac{\phi_{kr}}{\omega_r^2 - \omega^2 + i\eta_r\omega_r^2}\{\phi\}_r \tag{2}$$

In the following section it will be shown that the k th FRF shape is nothing but the k th column of dynamic flexibility matrix, i.e. k th dynamic flexibility shape.

In general, the equation of motion of a n DOF system with mass, stiffness and structural damping matrices of M, K and D is:

$$M\ddot{u}(t) + (K + iD)u(t) = f(t) \tag{3}$$

Consider a time-varying $n \times 1$ displacement response vector, $u(t)$, caused by an arbitrary applied force vector. Then the displacement vector at time t can be spanned by mode shapes as:

$$u(t) = q_1(t)\{\phi\}_1 + q_2(t)\{\phi\}_2 + \cdots + q_n(t)\{\phi\}_n \tag{4}$$

where the scalar $q_i(t)$ is the i th modal contribution factor at time t. Equation (4) can be written in matrix form

$$u(t) = \begin{bmatrix} \phi_1 & \phi_2 & \cdots & \phi_n \end{bmatrix} \begin{Bmatrix} q_1(t) \\ q_2(t) \\ \vdots \\ q_n(t) \end{Bmatrix} = \Phi q(t) \tag{5}$$

Φ is an $n \times n$ matrix containing orthonormal mode shapes as its columns and $q(t)$ is a generalized modal contribution vector. After substituting (5) in (3), a premultiplication of Φ^T yields

$$\Phi^T M \Phi \ddot{q}(t) + \Phi^T (K + iD) \Phi q(t) = \Phi^T f(t) \tag{6}$$

Application of orthogonality conditions $\Phi^T M \Phi = I$ and $\Phi^T (K + iD) \Phi = diag(\omega_r^2 (1 + i \eta_r))$ yields a system of uncoupled single degree of freedom equations:

$$\ddot{q}_r(t) + \omega_r^2 (1 + i \eta_r) q_r(t) = \phi_r^T f(t) \tag{7}$$

A static flexibility shape corresponding to r th DOF is the displacement response of the system due to a unit load applied at r th DOF. To extend the concept of flexibility shape to dynamic case, the unit exciting load is assumed harmonic with frequency ω resulting in a frequency dependent flexibility shape. Neglecting the transient effects, steady state response to a unit harmonic load exerted in r th DOF can be written as

$$q_i(t) = \frac{\phi_{jr}}{\omega_r^2 - \omega^2 + i \eta_r \omega_r^2} \sin \omega t \tag{8}$$

Substituting (8) in (4), the amplitude of r th dynamic flexibility shape is

$$u_j = \sum_{r=1}^{n} c_{jr} \phi_r = \sum_{r=1}^{n} \frac{\phi_{jr}}{\omega_r^2 - \omega^2 + i \eta_r \omega_r^2} \phi_r$$
$$= \sum_{r=1}^{n} \frac{(\omega_r^2 - \omega^2) \phi_{jr}}{(\omega_r^2 - \omega^2)^2 - (\eta_r \omega_r^2)^2} \phi_r - i \sum_{r=1}^{n} \frac{\eta_r \omega_r^2 \phi_{jr}}{(\omega_r^2 - \omega^2)^2 - (\eta_r \omega_r^2)^2} \phi_r \tag{9}$$

which is the same as FRF shape in (2). In the special case of $\omega = 0$, the flexibility shape reduces to r th static flexibility column which is in agreement with dynamically measured flexibility formula presented in reference [13].

The main advantage of using FRF shapes in damage detection is that it contains higher frequency information, while mode shapes construct a truncated basis for structural response space.

As can be seen from equation (9), both real and imaginary parts of FRF shape are multiplicands of r th mode shape with frequency dependent coefficients. Since damage can be identified in mode shapes in the form of an abnormality, i.e. a discontinuity in the curvature of mode shape [14], imaginary and real parts of an FRF shape can be used for damage localization.

At the damaged node, FRF shapes exhibit a local nonsmoothness or curvature discontinuity. Gapped Smoothing Method (GSM) is implemented to quantify this behavior in each node. A Cubic polynomial is fitted to two neighbor points before and two after a specific node. Subtracting curve fitted prediction, $\bar{y}(i)$ and the

original value, $y(i)$ comes to definition of index δ_i indicating relative degree of nonsmoothness at node i.

Figure (1) shows schematics of GSM. Higher values in GSM indices indicate potential damaged sites when applying on residual FRF shapes.
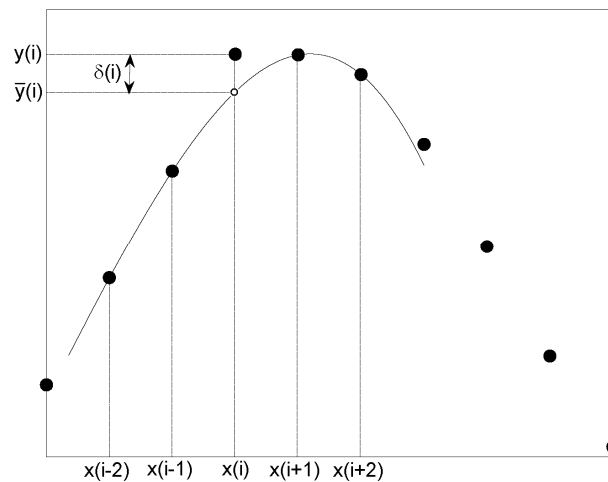

Fig. 1 calculation of GSM index at node i

Proposed method has several advantages over mode shape based methods. Firstly, damage detection is fulfilled over a wide frequency range rather than single resonance frequencies. Besides, great deal of modal analysis effort as well as errors induced by curve fitting is eliminated in this method.

To perform damage localization through this method, a single row (or column) of FRF matrix is needed. Trying with several FRF matrix rows can be used to increase reliability of the process.

3 Numerical case study

A 0.9m length aluminum cantilever beam of cross section 6.5mm×25.5mm is descretized by 80 two dimensional beam elements each have six degrees of freedom. Damage is simulated trough reducing the thickness of element 20 by 7.7 percent. Due to complicated nature of damping, it was decided to deal with it in experimental case study in which damping is present in its realistic form. Harmonic analysis has been carried out by applying input force at node 21 in the frequency range of 0 to 500 Hz with 0.1Hz frequency increment for both intact

and damaged structures. Five flexural modes are available in this frequency range. Natural frequencies of both intact and damaged beams are tabulated in Table (1).

Table 1: Natural frequencies of healthy and damaged beams

Mode	1	2	3	4	5
healthy (Hz)	6.58	41.37	115.62	226.58	374.34
damaged (Hz)	6.53	41.03	114.99	226.03	373.12

To simulate real test situations where measurement of all DOFs, especially rotational ones, is difficult, all displacement data except for the transverse vibrations are thrown away.

Some FRF shapes at different frequency points are depicted in Figure (2).
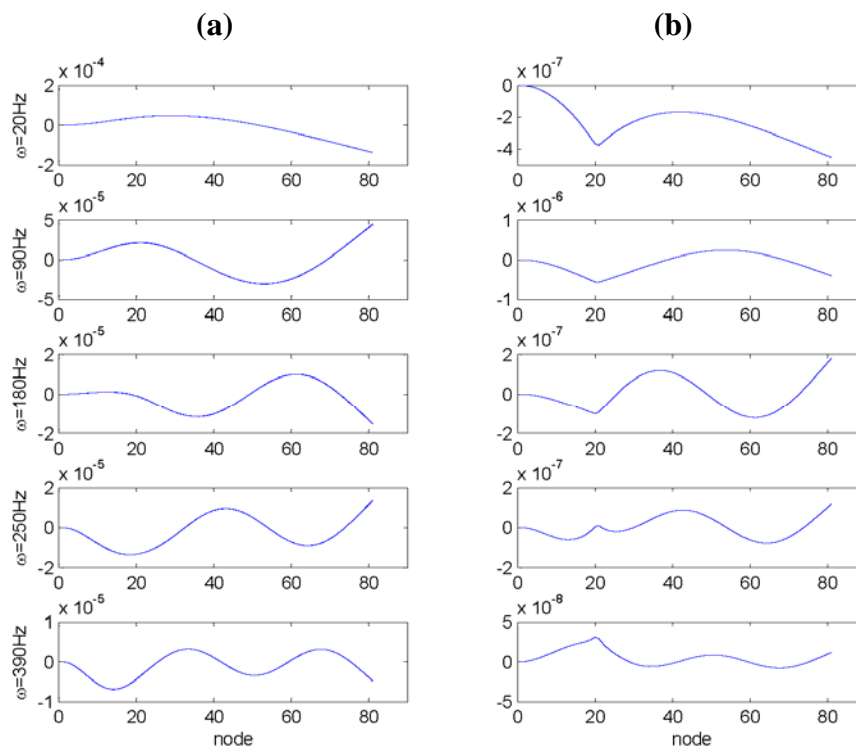
Fig. 2 (a) FRF shapes of healthy (solid line) and damaged (dashed line) at some various frequencies (b) corresponding residual FRF shapes

GSM is applied on the residual FRF shapes i.e. difference of intact and damaged state FRF shapes at each frequency point. Figure (3) shows the

normalized damage indices along frequency range of analysis which indicates damage in element 20 clearly.
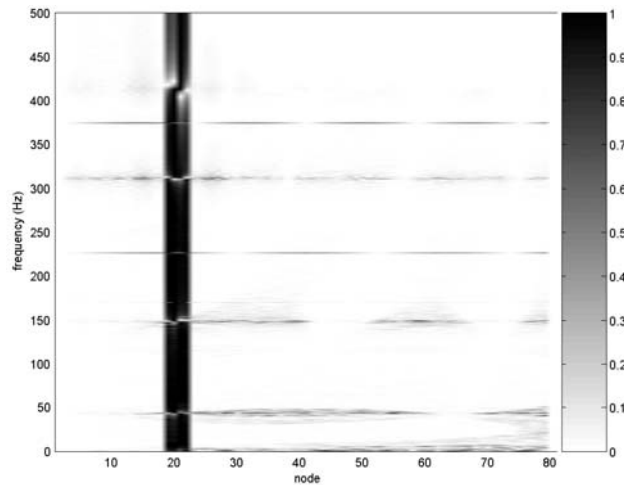

Fig. 3 GSM indices in frequency range of excitation

In realistic situations, measuring such dense grid points is impractical. To evaluate the effectiveness of the method in practical point of view, measuring nodes are reduced to 21. The new damage indication diagram is depicted in Figure (4). As can bee seen, the results are satisfactory.
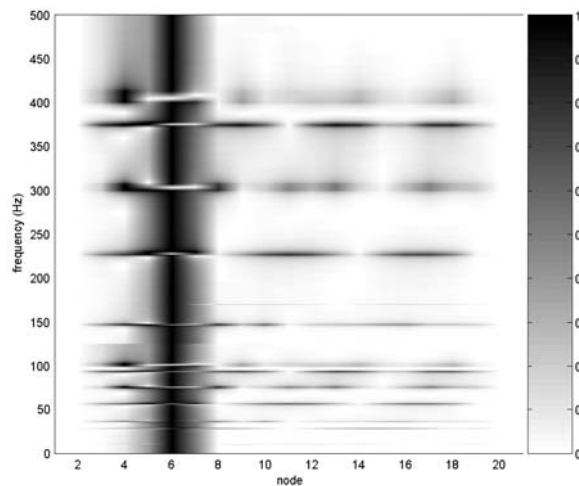

Fig. 4 GSM indices in frequency range of excitation in reduced measurement points case

Similar results are reported by Liu, Lieven and Ambrosio using imaginary parts of FRF shapes [14]. Perhaps the near zero amplitude of real parts of FRF shapes at resonant frequency makes one discouraged to apply real parts in a damage detection scheme. However, the numerical case study exhibits satisfactory results.

4 Experimental case study

To verify the proposed method from practical point of view, modal test were carried out on a rectangular cross section aluminum beam. Test has been carried out in free-free condition by suspending the test object by some elastic bungees. The beam is of cross section 50mm×25mm and 800 millimeters length. Seventeen equally spaced measurement points were marked on the beam. The test was carried out in the frequency range of 0 to 1600 Hz with frequency steps of 0.5 Hz. A B&K 8202 hammer with metal tip was used to excite the structure and acceleration response was measured by a PCB 356B08 accelerometer in vertical direction. The FFT analyzer used to carry out and process the frequency response functions were B&K Portable PULSE 3560D. Figure (5) shows the experimental setup.
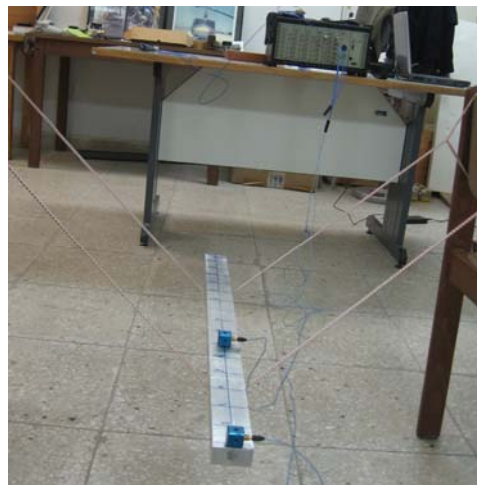

Fig. 5 Experimental test setup

Damage is simulated through making an artificial slot of depth 10 millimeters over the width of the beam at node 7. Measured FRFs corresponding to various excitation points and response at node 7 for healthy beam are shown in Figure (6).
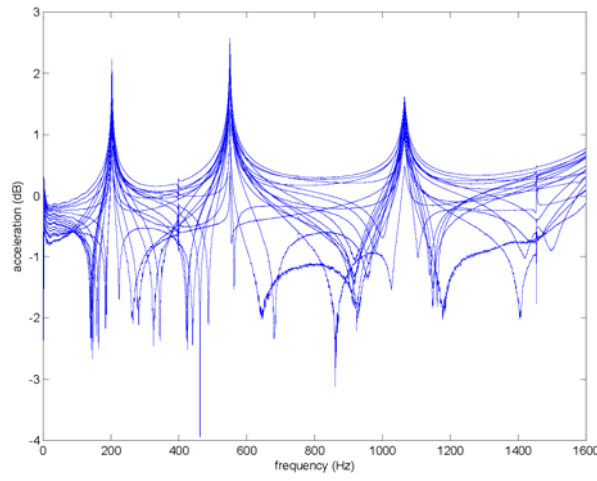
Fig. 6 Measured FRFs in healthy case

Resonance frequencies of the structure in both healthy and damaged states are shown in Table (2).

Table 2: natural frequencies of healthy and damaged aluminum beams

Mode	1	2	3
Healthy (Hz)	201.7	549.6	1063.4
Damaged (Hz)	177.6	513.2	1054.4

Figure (7) shows normalized GSM indices along frequency range of excitation for real part of FRF shapes. Damage at node 7 is evidently detectable from the figure.
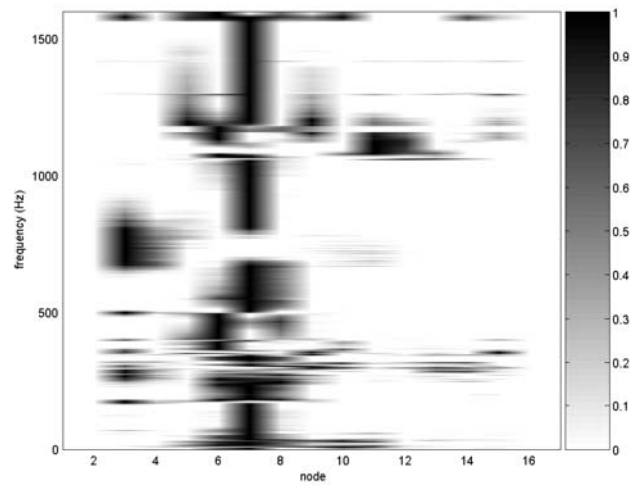

Fig. 7 GSM indices corresponding to real FRF shapes of aluminum beam

Using imaginary part of residual FRF shapes results less indicative results. Figure (8) depicts the GSM indices.
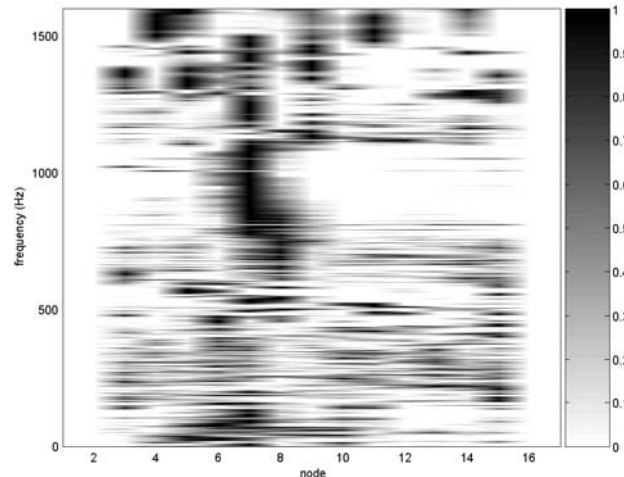

Fig. 8 GSM indices corresponding to imaginary FRF shapes of aluminum beam

In contrast to Liu's findings [6], it can be concluded, at least in presented experimental case study, that using real part of residual FRFs comes to more reliable results.

5 Conclusion

A non model based method of structural damage localization using frequency response function data was presented. The method verified by numerical case study successfully. The experimental case study works well when using real part of FRF shapes, but the results are less indicative utilizing imaginary part. The proposed method has the advantage of using measured FRFs directly without any need to perform modal analysis.

References

[1] P. Cawley and R.D. Adams, The location of defects in structures from measurements of natural frequencies, Journal of Strain Analysis, vol. 14, 49–57, 1979.

[2] D.J. Ewins, Modal testing: Theory, practice and application, Second Edition, Research Studies Press, 2000.

[3] H. Guan and V.M. Karrbhari, Improved damage detection method based on element modal strain damage index using sparse measurement, Journal of Sound and Vibration, vol. 309, 465-494, 2008.

[4] B. Jaishi and W.X. Ren, Damage detection by finite element model updating using modal flexibility residual, Journal of Sound and Vibration, vol. 290 , 369-387, 2006.

[5] N.A.J. Lieven and D.J. Ewins, Spatial correlation of mode shapes, the Coordinate Modal Assurance Criterion (COMAC), in: Proceedings of the Sixth International Modal Analysis Conference, Vol.1, 1988, 690– 695.

[6] X. Liu, N.A.J. Lieven and P.J. Escamilla-Ambrosio, Frequency response function shape-based methods for structural damage localization, Mechanical Systems and Signal Processing, vol. 23, 1243-1259, 2009.

[7] Q. Lu, G. Ren and Y. Zhao, Multiple damage location with flexibility curvature and relative frequency change for beam structures, Journal of Sound and Vibration, vol. 253, 1101-1114, 2002.

[8] N.M.M. Maia, J.M.M. Silva and R.P.C. Sampaio, Localization of damage using curvature of the frequency response functions, in: XV International Modal Analysis Conference, Orlando, USA, 1997, 942-946.

[9] A.K. Pandy, M. Biswas and M.M. Samman, Damage detection from changes in curvature mode shapes, Journal of Sound and Vibration, vol. 145 , 321– 332, 1991.

[10] R. Perera and A. Ruiz, A multi-stage FE updating procedure for damage identification in large scale structures based on multi-objective evolutionary optimization, Mechanical Systems and Signal Processing, vol. 22 , 970-991, 2008.

[11] M. Salehi, and S. Ziaei-Rad, Ground vibration test (GVT) and correlation analysis of an aircraft structure model, Iranian Journal of Science and Technology, Transaction B:Engineering, vol. 31, 65-80, 2007.

[12] M. Salehi, S. Ziaei-Rad and M. Ghayour, A structural damage detection technique based on modal strain energy, Proceeding of 17th Annual (International) Conference on Mechanical Engineering ISME2009, 19-21 May, Tehran, Iran, 2009.

[13] R.P.C. Sampaio, N.M.M. Maia and J.M.M. Silva, Damage detection using the frequency response function curvature method, Journal of Sound and Vibration, vol. 226, pp. 1029-1042, 1999.

[14] H. Sohn, C.R. Farrar, F.M. Hemez, D.D. Shunk, S.W. Stinemates, B.R. Nadler and J.J. Czarnecki, A review of structural health monitoring literature from 1996-2001, Los Alamos National Laboratory Report, Technical Report LA-13976-MS, 2004.

[15] W.M. West, Illustration of the use of modal assurance criterion to detect structural changes in an orbiter test specimen, in: Proceedings of the Air Force Conference on Aircraft Structural Integrity, 1984, 1-6.